Article

Numerical and Experimental Investigation on the Effect of Mechanical Smoke Extraction Caused by External Wind in Subway Station Halls

Jiali Liu [1], Xianwang Fan [1], Bei Wang [2], Tianzhen Ye [1,3,*], Zhangxiang Wu [1] and Enzhong Xing [1]

1   School of Environmental Science and Engineering, Tianjin University, Tianjin 300350, China
2   Tianjin Anjie IoT Science And Technology Co., Ltd., Tianjin 300392, China
3   National Engineering Research Center for Digital Construction and Evaluation of Urban Rail Transit, Tianjin 300350, China
*   Correspondence: tzhye@tju.edu.cn

Abstract: When fires break out in subway station halls, traditional smoke extraction (TSE) systems are employed with the aim of preventing smoke from spreading to the platform and passageways. The functionality of TSE systems under the influence of external winds needs to be further explored. Based on a numerical method, this study investigated the effect on TSE systems under the influence of external wind. A numerical model was established and validated by means of full-scale field tests to ensure accuracy. Subsequently, the validated model was applied to study the effect of the external wind directions and speeds on the smoke diffusion distance. The results showed that when all entrances and exits were on the windward side, the external wind direction led to serious longitudinal diffusion of the smoke toward the side with fewer entrances and exits of the station hall, and the diffusion distance increased with increasing wind speed. The diffusion distance reached a maximum value of 61.32 m when the outdoor wind was 5 m/s, which was 67.9% higher than that under no wind. When all the entrances and exits were on the leeward side, the external wind had little influence on the degree of smoke spread, with the greatest smoke diffusion distance being only 4.76% longer than that under no wind. When two entrances and exits were on the windward side and the other on the leeward side, the external wind caused smoke to spread to a passageway, and the degree of smoke spread was more unfavorable at higher wind speeds, with the longest diffusion distance being 7.28 m. To prevent smoke from spreading to passageways and to effectively shorten the longitudinal diffusion distance of smoke, an optimized smoke control (OSC) system was proposed, employing center and passageway smoke barriers, which were able to shorten the diffusion distances by 35.45%, 13.64%, and 2.35%. In particular, smoke diffusion did not occur in passageways. This study provides a reference for the fire safety engineering design of subway stations.

Keywords: external wind; numerical method; full-scale test; smoke control system

1. Introduction

Subways have gradually become an important means of public transportation in cities, having the benefits of low cost and accurate operating times [1]. By the end of 2021, there were 283 operation lines and 5343 stations for urban rail transit in 50 cities in China, of which subways accounted for 78.3% [2]. A subway station has a narrow and semi-closed spatial structure and dense personnel flow, and in the event of a fire outbreak, this can lead to the problem of suffocation and the difficulty of evacuation when the smoke from the fire cannot be discharged in a timely fashion. The problem of smoke spread should be a significant point of focus, because more humans die from smoke suffocation than from burning [3].

In the case of fires in station halls, the entrances and exits for escape provide fresh air to the station hall. Tianjin has a typical temperate and monsoonal climate, with monsoon

prevailing. If the external wind enters these entrances and exits, the smoke flow within the station hall, and, thus, the efficacy of the TSE system, will be affected. However, smoke diffusion can be effectively controlled by optimizing the TSE system, thus reducing the exposure of passengers to excessive smoke and providing guaranteed life safety. Therefore, it is important to study the influence of external wind on smoke in the station hall.

The driving forces of smoke spread mainly include thermal buoyancy, external wind, and mechanical ventilation [4]. Some scholars have studied fire in subway stations on the basis of experiments. Chen et al. [5] optimized a smoke exhaust scheme under various heat release rates and fire source positions using a 1:10 fire experiment model of a metro station. Wu et al. [6] identified the change laws for the settlement time and temperature of smoke in a station hall within 6 min of the commencement of a fire on the basis of experiments and numerical methods. Zhao et al. [7] investigated the efficacy of different ventilation modes for smoke control and proposed an optimized ventilation mode. Long et al. [8] conducted full-scale experiments to investigate the height of the smoke layer and the maximum temperature near the fire source in a station hall under natural and mechanical ventilation. Gao et al. [9] analyzed the effect of mixed ventilation on reducing the CO concentration and inhibiting the horizontal dispersion of smoke. Based on the Froude number, Giachetti et al. [10,11] established a scale model experimental platform for subway stations, and studied the relationship between thermal upwelling, transverse flow, and the potential chimney effect. They determined the most effective ventilation mode for preventing the diffusion of smoke into the evacuation passages.

Some scholars have studied fire in subway stations by means of numerical simulation. Zhong et al. [12] studied the smoke flow characteristics of a station hall fire under the combined action of piston wind, thermal buoyancy, and mechanical ventilation using Fluent. Roh et al. [13] conducted a simulation of a fire and evacuation in order to assess the impact of PSDs (platform screen doors) and ventilation systems on the safety of passengers' lives in the context of a subway train fire. Tsukahara et al. [14] simulated and calculated the behavior, temperature, and CO and CO_2 concentrations of flue gas at Daegu Fire Station in order to determine the most effective evacuation route for the subway station via FDS. Park [15] also used the FDS program to study the ventilation and smoke movement characteristics of the subway station platform, and verified the numerical model based on the actual subway station test. The influence of smoke discharge on hot smoke movement was investigated. It can be seen that the previous research has largely been focused on the influence of the fire source and the mode of ventilation on the diffusion of smoke and the TSE system, while few studies have considered external wind as a factor.

Zhong et al. [16] discovered that the smoke descending in the region downwind of the fire source was significantly influenced by natural wind, and further demonstrated that the spatial layout of the exits and the suspended ceiling should be comprehensively considered in order to utilize natural wind pressure. Tian et al. [17] indicated that the diffusion of smoke through the station hall was effectively limited as a result of the influence of natural winds at the entrances and exits. Long et al. [18] found that the natural wind pressure from north to south made the north entrance less dangerous, and smoke did not spread into the connecting passageways and platforms when the station hall caught fire. They only considered a specific external wind, and did not conduct comprehensive studies on external wind with a quantitative analysis of different wind directions and speeds.

As a result, the trends of the external wind direction and wind speed in Tianjin were first organized in this study. The compiled UDF file was used to calculate the external wind gradient wind speed, and a volumetric heat source model was utilized to simplify the fire source. A numerical simulation was conducted to analyze the characteristics of smoke spread and the impact of external wind on the TSE system of the station hall under different external wind directions and speeds. In addition, a numerical model was developed and validated using data from full-scale field testing [19]. It was found that different wind directions influenced the smoke spread trend, whilst different wind speeds influenced the distance of smoke spread. The numerical simulation results showed that the smoke

was dispersed into the passageway by the external wind, and the station hall had a longer longitudinal diffusion distance of smoke. Therefore, the OSC system of the station hall was considered and analyzed while taking into account the impact of external winds.

2. Modeling and Experimental Validation

2.1. Numerical Method

A full-scale geometric model was established based on an actual Tianjin Metro Line 1 subway station, which portrays a typical subway station with smoke extraction systems. Figure 1 shows the three-dimensional computation domain used to simulate the outside flow field, with dimensions of 324 m × 324 m × 10 m. The subway station hall was regarded as the center of the outside flow field, and each side of the outdoor flow field was three times the station's maximum diameter [20]. The height of the outdoor flow field was a standard height [21], and the blockage ratio of the windward part at the entrance and exit was less than 3% [22]. The passageways connected the station hall with the external environment, with passageways A and C facing south and D facing east, respectively. The dimensions are listed in Table 1. The computational domain of this study included the subway station hall and the outdoor flow field.
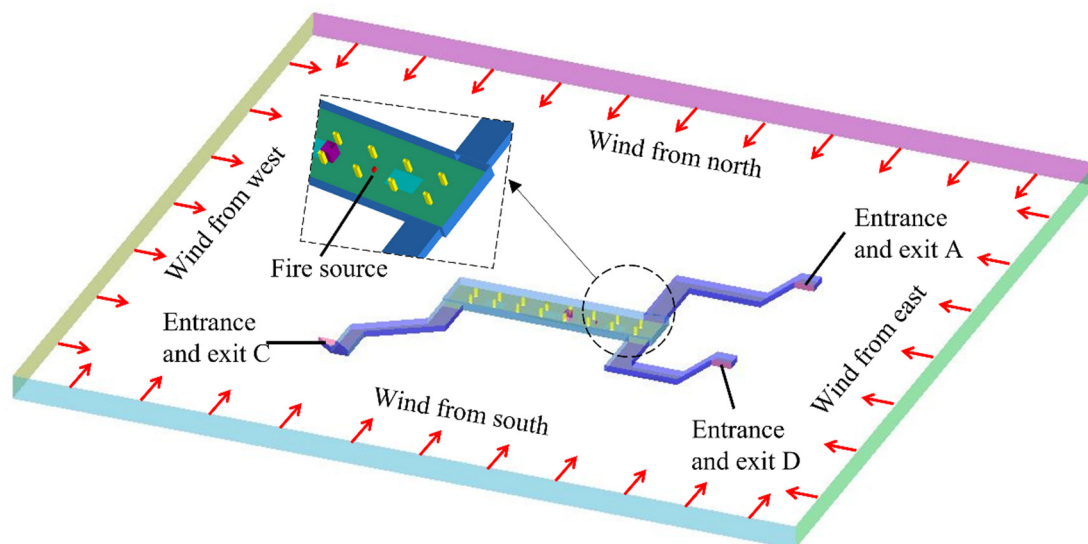

Figure 1. Geometrical model of the subway station.

Table 1. Dimensions of the station hall.

Composition	Length (m)	Width (m)	Height (m)	Direction
Outdoor flow field	324.0	324.0	10.0	-
Station hall	86.6	9.1	3.5	-
Supply outlet	0.4	0.4	-	-
Exhaust outlet	0.4	0.4	-	-
Passageway A	82.6	8.0	2.6	South
Passageway C	85.0	6.2	2.6	South
Passageway D	74.0	8.0	2.6	East

The ventilation system of the station hall consisted of two exhaust ducts and two air supply ducts. There were 40 air outlets with a diameter of 0.4 m for each air duct, of which the magenta lines represent the exhaust ducts and the cyan lines represent the air supply ducts, as shown in Figure 2a. During the normal operation of the station hall, a form of air distribution consisting of top air supply and return was employed. When fire occurred in the station hall, the air exhaust ducts were used as the smoke exhaust ducts. To discharge

smoke, the air handling unit was turned off and the air exhaust fan was replaced with a smoke extraction fan.
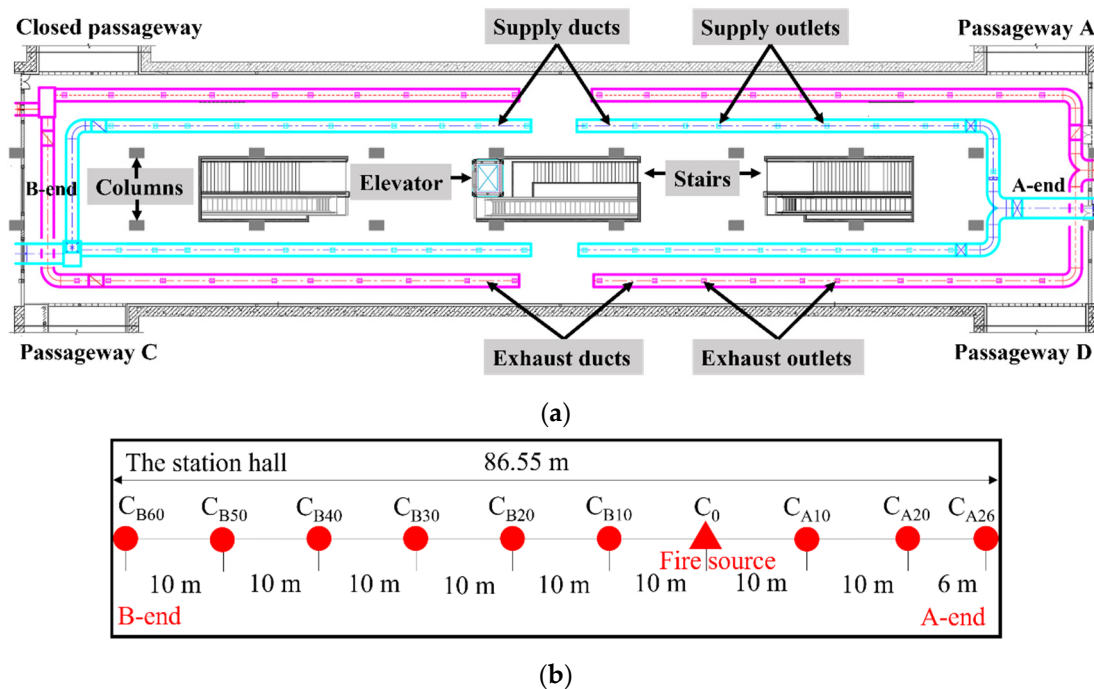
Figure 2. (**a**) Schematic of the station hall and (**b**) layout of the monitoring points.

The side of the station hall corresponding to passageways A and D was dubbed A-end, while the side corresponding to passageway C was dubbed B-end. With the fire source as the center, nine monitoring points were equidistantly arranged on both sides of A-end and B-end to monitor the variation in CO_2 concentration in real time, as illustrated in Figure 2b. The CO_2 concentration monitoring points are represented by C_{An} or C_{Bn}.

In this study, all analyses were performed using Fluent 2020 R2 version, and the finite volume method was utilized to discretize the governing equations. Specifically, a pressure-based solver was selected for the numerical method, and the SIMPLE scheme was used to couple velocity and pressure. The second-order upwind scheme was applied to solve the pressure, the momentum equation, the energy equation, and the species mass-conservation equation. Similarly, the first-order upwind scheme was applied to solve turbulent kinetic energy and turbulent dissipation rate. The residual of the governing equations should be less than 10^{-5}. In particular, the residual of the energy equation should be smaller than 10^{-6}.

To investigate the sensitivity of time steps, the average velocity at the entrances and exits was simulated using three time step sizes of 0.4 s, 0.2 s, and 0.1 s. The results demonstrate that there was minimal change between the wind speeds of 0.2 s and 0.1 s. However, the calculation time would grow by 2.8 times when the time step size was reduced from 0.2 s to 0.1 s. As a result, the time step size of 0.2 s was used throughout the entire simulation.

2.1.1. Assumptions

The following assumptions were utilized to simplify the numerical model:

(1) The walls of the subway station were adiabatic.
(2) The air in the subway station was assumed to be incompressible and to meet the Boussinesq hypothesis [23], and the physical properties of air were assumed to remain constant.

(3) The combustion process in the station hall was oxygen-enriched, and the combustion product was CO_2.

(4) The initial flow field in the subway station was steady.

2.1.2. Governing Equations

The main governing equations include the conservation equations for mass, momentum, energy, and component mass [24].

(1) Continuity equation

$$\frac{\partial \rho}{\partial t} + div(\rho \vec{v}) = 0. \tag{1}$$

(2) Momentum conservation equation

$$\frac{\partial(\rho u)}{\partial t} + div\left(\rho u \vec{v}\right) = div(\mu grad u) - \frac{\partial p}{\partial x} + S_u, \tag{2}$$

$$\frac{\partial(\rho v)}{\partial t} + div\left(\rho v \vec{v}\right) = div(\mu grad v) - \frac{\partial p}{\partial y} + S_v, \tag{3}$$

$$\frac{\partial(\rho w)}{\partial t} + div\left(\rho w \vec{v}\right) = div(\mu grad w) - \frac{\partial p}{\partial z} + S_w. \tag{4}$$

(3) Energy conservation equation

$$\frac{\partial(\rho T)}{\partial t} + div\left(\rho \vec{v} T\right) = div(\frac{\lambda}{c_p} grad T) + \frac{S_T}{c_p}. \tag{5}$$

(4) Species mass-conservation equation of components

$$\frac{\partial(\rho C_s)}{\partial t} + div\left(\rho C_s \vec{v}\right) = div[D_s grad(\rho C_s)] + S_s. \tag{6}$$

The flow of air and smoke has the obvious characteristic of high Reynolds number turbulence. The standard $k - \varepsilon$ two-equation turbulence model was introduced, and the finite volume method was used to solve the governing equations [25]. The turbulent viscosity η_t can be derived from the $k - \varepsilon$ calculation model as [26]

$$\eta_t = C_\mu \rho \left(\frac{k^2}{\varepsilon}\right). \tag{7}$$

The k equation is expressed as

$$\rho \frac{\partial k}{\partial t} + \rho u_j \frac{\partial k}{\partial x_j} = \frac{\partial}{\partial x_j}\left[\left(\eta + \frac{\eta_t}{\sigma_k}\right)\frac{\partial k}{\partial x_j}\right] + \eta_t \frac{\partial u_i}{\partial x_j}\left(\frac{\partial u_i}{\partial x_j} + \frac{\partial u_j}{\partial x_i}\right) - \rho\varepsilon. \tag{8}$$

The ε equation is expressed as

$$\rho \frac{\partial \varepsilon}{\partial t} + \rho u_k \frac{\partial \varepsilon}{\partial x_k} = \frac{\partial}{\partial x_k}\left[\left(\eta + \frac{\eta_t}{\sigma_\varepsilon}\right)\frac{\partial \varepsilon}{\partial x_k}\right] + \frac{C_{1\varepsilon}}{k}\eta_t \frac{\partial u_i}{\partial x_j}\left(\frac{\partial u_i}{\partial x_j} + \frac{\partial u_j}{\partial x_i}\right) - C_{2\varepsilon}\rho \frac{\varepsilon^2}{k}, \tag{9}$$

where $C_{1\varepsilon} = 1.44$, $C_{2\varepsilon} = 1.92$, $C_\mu = 0.09$, $\sigma_k = 1.00$, and $\sigma_\varepsilon = 1.30$ [27].

2.1.3. Initial and Boundary Conditions

Fluent was used to calculate the smoke flow and CO_2 concentration distribution characteristics of the station hall [28]. This study concentrated on the smoke concentration distribution surrounding the fire source rather than on the precise combustion process at the fire source. Therefore, a volumetric heat source model of 1 m × 1 m × 0.5 m was used to simulate the fire source combustion [29].

The location of the fire in the station hall is uncertain, but fires are more likely to occur in regions with dense personnel flow and narrow spaces, such as exits and staircases, which will have more significant consequences [30]. This study focused on the impact of external wind on smoke diffusion. The fire source was placed near the stairs at the A-end to observe the impacts of external wind and the TSE system on smoke.

Ref. [31] showed that luggage was the primary cause of fires in subway stations, and a constant fire source was utilized with a heat release rate of 2.5 MW. As stated in Appendix A, the outdoor gradient wind speed was achieved by introducing a UDF file into Fluent [32].

According to the requirements in ref. [33], the passengers on an oncoming train and the waiting personnel on the platform must be evacuated from the platform to reach the safety zone within 6 min after a fire occurs. The initial and boundary conditions in the simulation were obtained based on the field test and the model size, as listed in Table 2. The initial CO_2 concentration was 350 ppm, which corresponded to the general concentration of CO_2 in natural air, and the field test values were also around this value. The initial indoor air temperature, initial wall temperature, wind speed of the stairs leading to the platform, and outside air temperature were measured in our field. The wind speed of the exhaust outlet was calculated by the exhaust air rate and was also checked on the spot.

Table 2. Initial and boundary conditions of the simulation.

Single Valued Condition	Value
Initial CO_2 concentration (ppm)	350
Initial indoor air temperature (°C)	22.3
Initial wall temperature (°C)	21.6
Outside air temperature (°C)	13.7
Wind speed of stair section (m/s)	1.57
Wind speed of exhaust outlet (m/s)	3.77

According to the parameters of typical meteorological years in ref. [34], the frequency of wind direction and speed in Tianjin, China, were counted in different seasons. Figure 3 displays a rose chart of wind direction over the full year, including summer (June to August), winter (December to February), and transition seasons (March to May and September to November). The dominant wind directions were southeast by south (SSE) in summer, north (N) in winter, and southwest (SW) in the transition season.

The annual wind speed range was 1.0-5.0 m/s, of which the range of 1.8-2.2 m/s accounted for 45.8%. Therefore, an external wind speed of 2.0 m/s was employed to investigate the effect of different external wind directions on the smoke spread characteristics. To analyze the impact of different external wind speeds, five wind speeds of 1, 2, 3, 4, and 5 m/s were considered under the same wind direction.
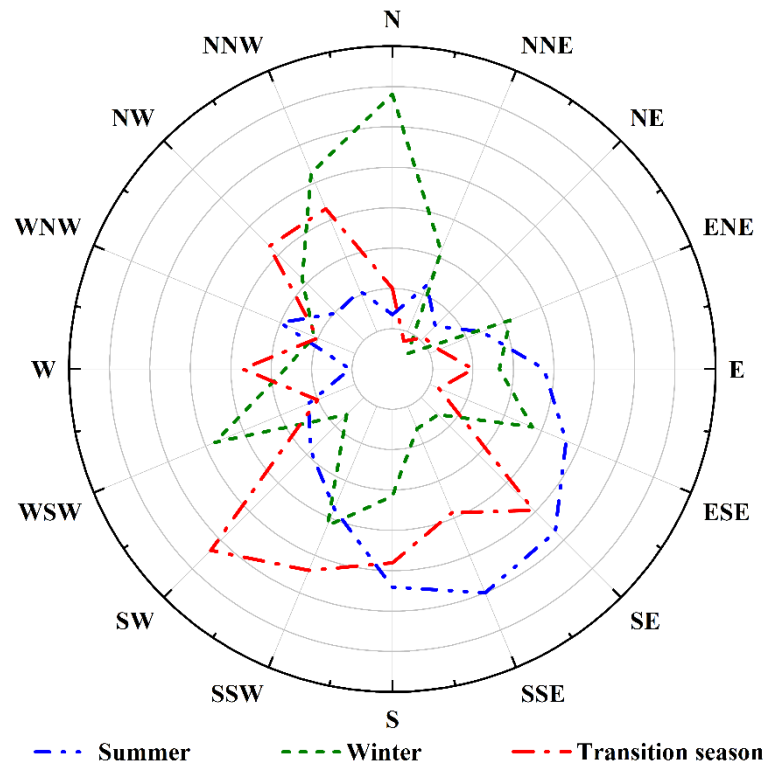
Figure 3. Wind direction rose chart in Tianjin.

2.1.4. Mesh Independence Examination

Due to the intricacy of the physical model, a tetrahedral grid was utilized to discretize the computational domain. Grids of 1.6 million, 3.38 million, 5 million, 6.67 million, and 8 million points were divided before the simulation to examine the independence of the grids. Figure 4a shows the average velocity at the entrances and exits of A, C, and D with a SW wind of 2 m/s. The wind speeds at the three entrances remained practically unchanged as the number of grid cells increased from five to eight million. Therefore, the model was divided into five million grids for subsequent calculations.
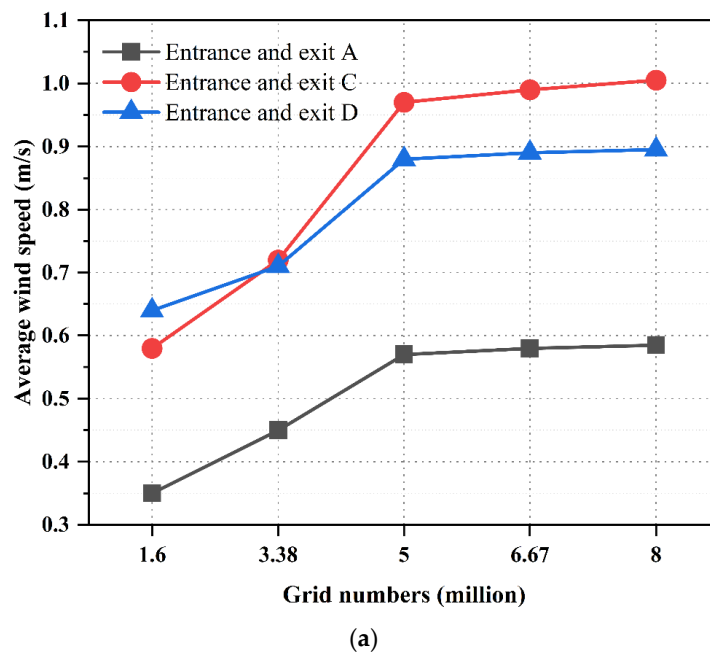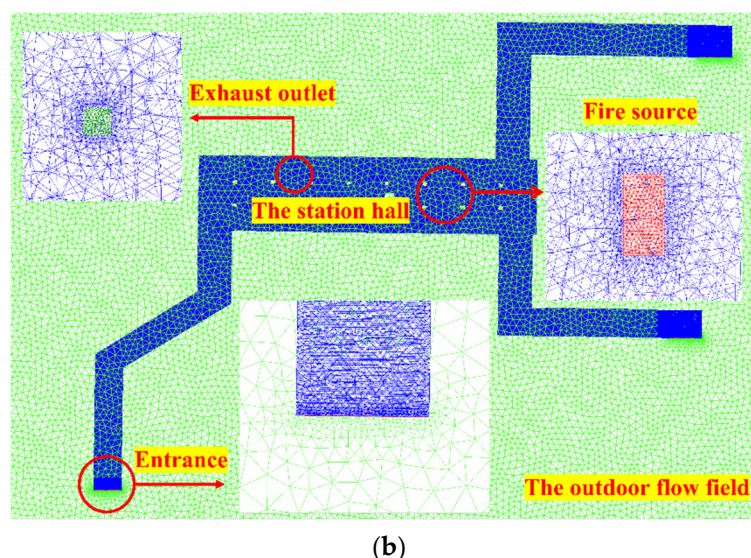

(**a**)

Figure 4. *Cont.*

(**b**)

Figure 4. Mesh of the model: (**a**) average wind speeds of different grid numbers, (**b**) grid detailing.

In Figure 4b, the maximum grid sizes of the outside flow field and the station hall were 2 m and 0.3 m, respectively. The grid was refined in regions with a high velocity gradient or concentration gradient, such as the entrances and exits of the station hall, exhaust outlets, and the fire source, with maximum sizes of 0.2 m, 0.04 m, and 0.05 m, respectively.

2.2. Model Validation

2.2.1. Field Tests

To obtain the single-value condition and validate the accuracy of the numerical model, full-scale field tests were conducted in May 2021 at the Tianjin Metro Line 1 subway station. The measurement points were placed in the station hall, passageways, and outside [35]. Temperature and humidity loggers were used to measure the air temperature. The wall surface temperature of the station hall was obtained using a data acquisition instrument and K-type thermocouples, the indoor air velocity was multi-point tested using hot-wire anemometers, and the outdoor wind speed and direction were measured using a portable weather station. The key test instruments are shown in Figure 5, and the important parameters are listed in Table 3. Moreover, all the instruments were calibrated prior to the field test. The temperature and humidity loggers were uniformly arranged on the columns of the station hall, the hot-wire anemometers were arranged on the exhaust vents and at three entrances and exits of the station hall, and the portable weather stations were placed near the subway station, 10 m above the ground.

Table 3. Test instrument and related parameters.

Parameters	Equipment Name	Range	Measurement Accuracy
Air temperature	Temp/RH logger	−20–70 °C	±0.21 °C
Wall temperature	Thermocouple	−50–300 °C	±0.15 °C
Indoor wind speed	Hot-wire anemometer	0–30 m/s	±0.1 m/s
Outdoor wind speed	Portable weather station	0–70 m/s	±0.1 m/s
Outdoor wind direction	Portable weather station	0–360°	±1°

The cold smoke test, which involves lighting a smoke cake to create smoke, has been conducted extensively, but cold smoke cannot adequately reflect the thermal buoyancy of the rising smoke. Therefore, in this investigation, a hot smoke test was carried out by combining burning alcohol with smoke cake, as illustrated in Figure 5e. The main product of the burning smoke cake was CO_2, and all the test data were recorded while the operation of the system was steady.
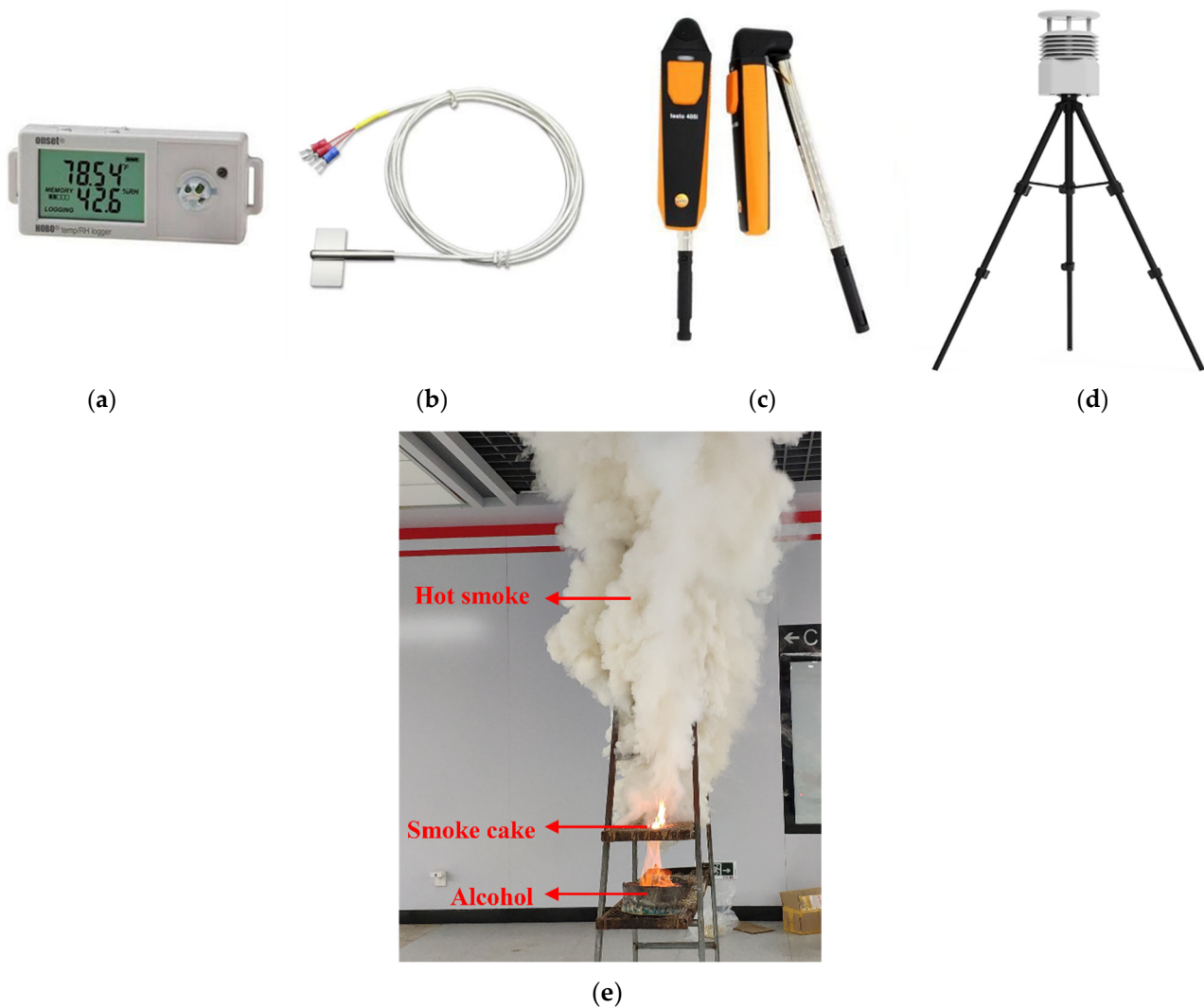
Figure 5. Main measuring instruments and fire source device: (**a**) temperature and humidity logger, (**b**) thermocouple, (**c**) hot-wire anemometer, (**d**) portable weather station, (**e**) design of the fire source device.

2.2.2. Validation of Velocity Field

To accurately reflect the actual wind speed, a multipoint measuring approach and an average value were adopted. The specific layout of the measuring points is shown in Figure 6, and data were recorded every 2 s. All test data were averaged over three measures to minimize the inaccuracy caused by unintentional variables. The uncertainty of measured wind speed can be estimated as

$$X_i = X_i(measured) \pm \delta X_i, \tag{10}$$

$$\sigma = \sqrt{\frac{\sum_{i=1}^{n}\left(X_i - \overline{X}\right)^2}{n-1}}, \tag{11}$$

where the value $X_i(measured)$ is the mean value of three set of repeated experiments, σ is the standard deviation of repeated experiment data and $\delta X_i = 2\sigma$ [36].
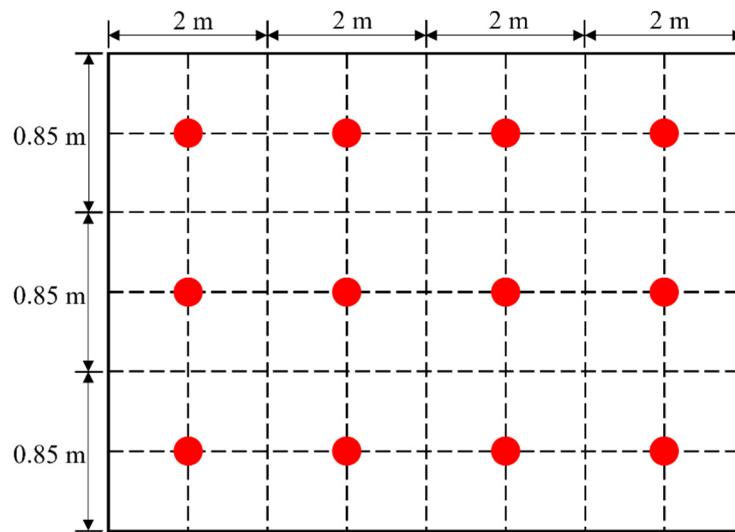
Figure 6. Schematic of the air velocity points at passageways.

Before the alcohol was lit, the initial air temperature and wall temperature were measured. When the portable weather station detected an external wind speed of more than 2 m/s, the alcohol was lit, and the smoke cake created smoke as well. At this time, the smoke exhaust system of the station hall was opened, and hot-wire anemometers continuously recorded the smoke speed of the entrances and exits of the station hall, exhaust outlets, and staircases leading to the platform.

Identical initial and boundary conditions as in the field test were used for the simulations, and velocity test values were used to validate the numerical model. The relative error between the experimental and numerical simulation results is defined as [37]

$$\delta = \frac{|V_{num} - V_{exp}|}{V_{exp}} \times 100\%. \tag{12}$$

As listed in Table 4, after activating the TSE system, the relative errors between the simulation and test values in passageways A, C, and D were 4.08%, 5.36%, and 8.57%, respectively. The errors were mainly caused by the simplification of the physical model. However, the maximum relative error was less than 10%, indicating that the numerical model is quite accurate in simulating smoke movement in the station hall.

Table 4. Comparison between simulation and test value.

Passageway	Simulation Value of Wind Speed (m/s)	Test Value of Wind Speed (m/s)	Mean Relative Error
A	0.51	0.49 ± 0.05	4.08%
C	0.59	0.56 ± 0.06	5.36%
D	0.38	0.35 ± 0.03	8.57%

3. Results and Discussions

The height of the smoke is thought to be a crucial factor in passenger evacuation. The safe smoke height was described in [37]:

$$H_s = 1.6 + 0.1H, \tag{13}$$

where 1.6 m represents the average height of passengers, and H is 3.5 m in the physical model established in this study. Therefore, H_s was determined to be 1.95 m. When the actual height of the smoke layer is higher than H_s, passengers can safely evacuate the subway station [38].

Butcher and Parnell [39] demonstrated that CO_2 in flames should be classified as a dangerous gas. The CO_2 volume fraction in natural air is typically 0.03–0.04% [40]. However, when the inhaled volume fraction of CO_2 exceeds 1.0%, a person's respiratory volume begins to rise; if the volume fraction of CO_2 rises further, it might cause dyspnea, headache, dizziness, coma, and death [41]. As a result, the CO_2 volume fraction limit was set at 1.0%, and the location in the station hall where the CO_2 volume fraction exceeded 1.0% at 1.95 m was designated as the smoke-diffusion area.

According to ref. [33], when smoke is emitted from the station hall, it should be prevented from entering neighboring places, such as the passageways of entrances and exits. Therefore, the smoke control system's role is to prevent smoke from spreading into the passageways, to decrease the longitudinal diffusion distance of smoke in the station hall as much as feasible, and to establish an evacuation atmosphere.

The impacts of the external wind direction and speed were analyzed using the findings of the working conditions listed in Table 5.

Table 5. Basic simulation conditions.

Case	External Wind Direction	External Wind Speed (m/s)
0	No wind	-
1	SSE	1
2	SSE	2
3	SSE	3
4	SSE	4
5	SSE	5
6	N	1
7	N	2
8	N	3
9	N	4
10	N	5
11	SW	1
12	SW	2
13	SW	3
14	SW	4
15	SW	5

3.1. No Wind

Figure 7 depicts the characteristics of the smoke concentration distribution under Case 0 to quantitatively assess the unique impacts of external wind on the TSE system, where the diffusion distance was 36.5 m and the smoke never passed the border into the passageways. The smoke diffusion was not substantial in Case 0, indicating that the TSE system was appropriate.
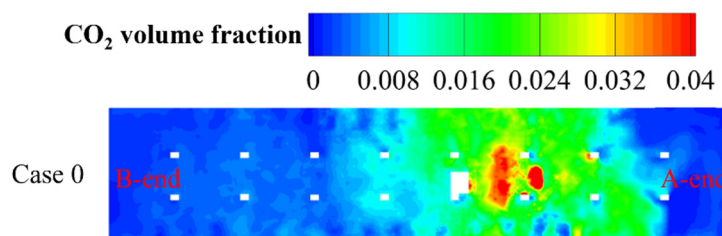
Figure 7. Smoke concentration distribution characteristics in the station hall under Case 0.

3.2. Influence of External Wind

3.2.1. SSE Wind

All entrances and exits were on the windward side when the external wind direction was SSE. Figure 8 shows the smoke concentration distribution characteristics with time

and pressure distribution characteristics at 360 s in the station hall under the Case 2 condition. In Figure 8a, the smoke concentration distribution contours indicate the spread of smoke toward B-end overtime. According to Figure 8b, smoke moved sequentially to the monitoring points C_{B10}-C_{B60}, and the related concentrations gradually rose over time, but the smoke concentrations at monitoring points C_{A10} and C_{A20} increased and subsequently declined. This was due to the smoke being less impacted by the external wind in the first 90 s, when it expanded to both sides with the fire source as the center at the same time. The smoke spread toward A-end was restricted after the external wind reached a constant wind speed, while the smoke spread to B-end was aided by the SSE wind.
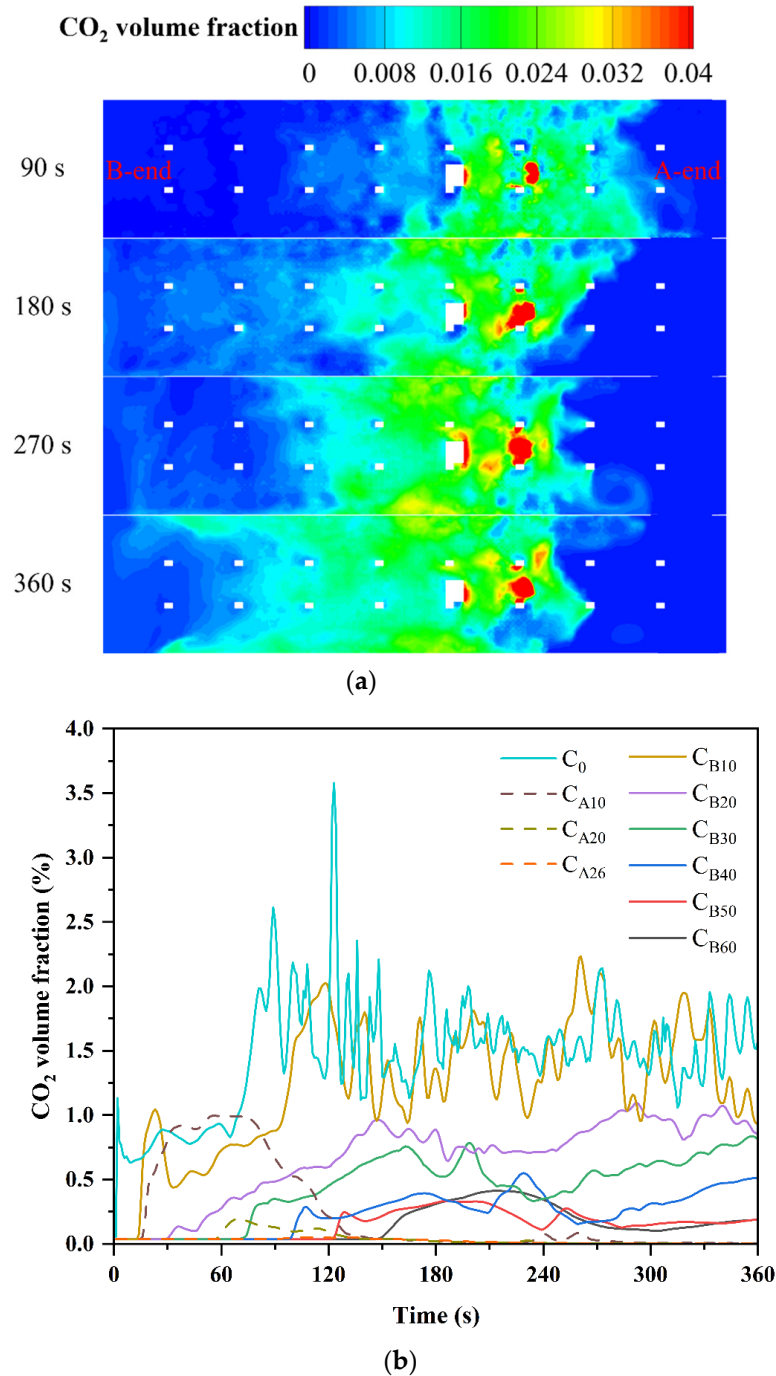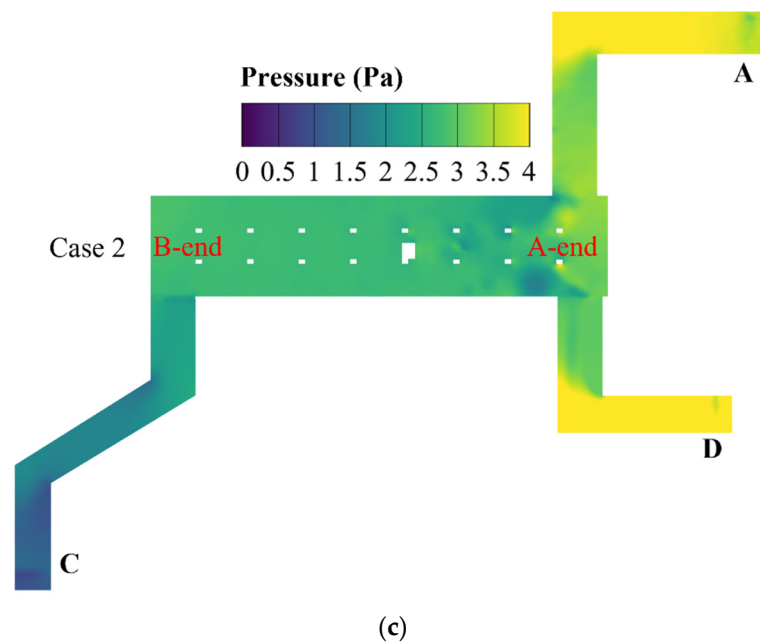

(a)

(b)

Figure 8. *Cont.*

(**c**)

Figure 8. Smoke concentration distribution characteristics with the time and pressure distribution contour in the station hall under Case 2. (**a**) Distribution contours, (**b**) variation at the monitoring points, (**c**) pressure distribution contour at 360 s.

A further analysis of the pressure distribution contour is shown in Figure 8c. The external wind entered the station hall through the three entrances and exits, which were determined by the orientation. However, because passageways A and D were on the same side, the positive pressure created by the external wind entering the station hall on this side was larger than the positive pressure created by passageway C. As a result of the pressure gradient, the smoke in the station hall spread to the B-end. When the flow field was steady, the values of wind speeds in passageways A, C, and D were 0.41 m/s, 0.36 m/s, and 0.70 m/s, respectively.

Under the SSE wind direction, five typical working conditions were simulated, with wind speeds ranging from 1 to 5 m/s. Figure 9 shows the smoke concentration distribution characteristics of the station hall. In Figure 9a, the CO_2 concentration distribution contour displays that the smoke spread to B-end increased with increasing wind speed. The highest CO_2 concentration values along the longitudinal direction of the station hall were extracted, as shown in Figure 9b, and the concentration distribution curves of the station hall were produced under different external wind speeds. The CO_2 concentration was greatest around the fire source. The value of CO_2 concentration progressively fell as the external wind speed rose, and the SSE wind resulted in a peak value closer to the B-end compared to that in Case 0; the concentration of the smoke at the B-end steadily increased at the same time. Therefore, the smoke moved to the B-end due to the SSE wind.

As shown in Figure 9c, the longitudinal diffusion distance of smoke rose with rising external wind speed, indicating that the high SSE wind speed aggravated the degree of longitudinal spread to the B-end. The greatest longitudinal diffusion distance of 61.3 m was attained with a wind speed of 5 m/s, representing a 67.9% increase over Case 0. Hence, the smoke control capability of the TSE system was reduced for the SSE wind direction, and the wind speed affected the smoke diffusion distance.
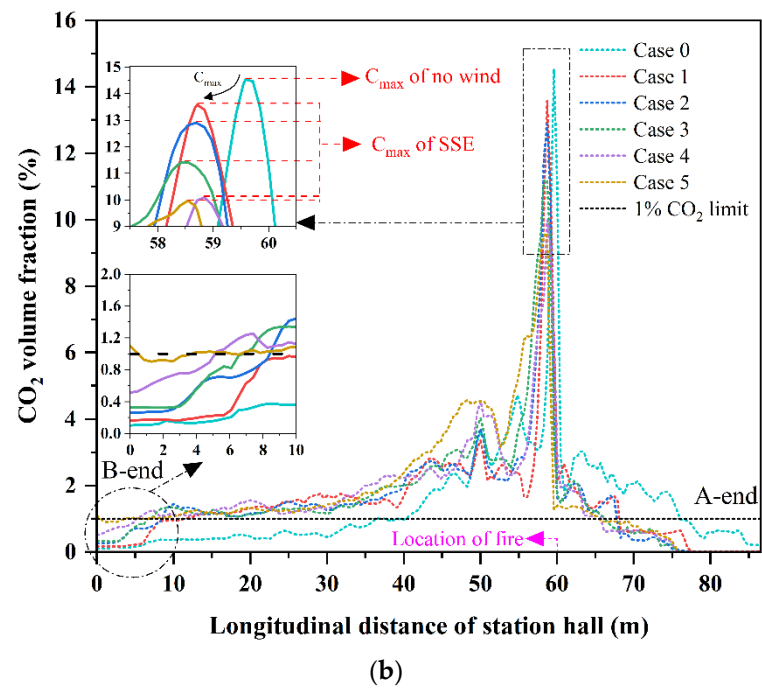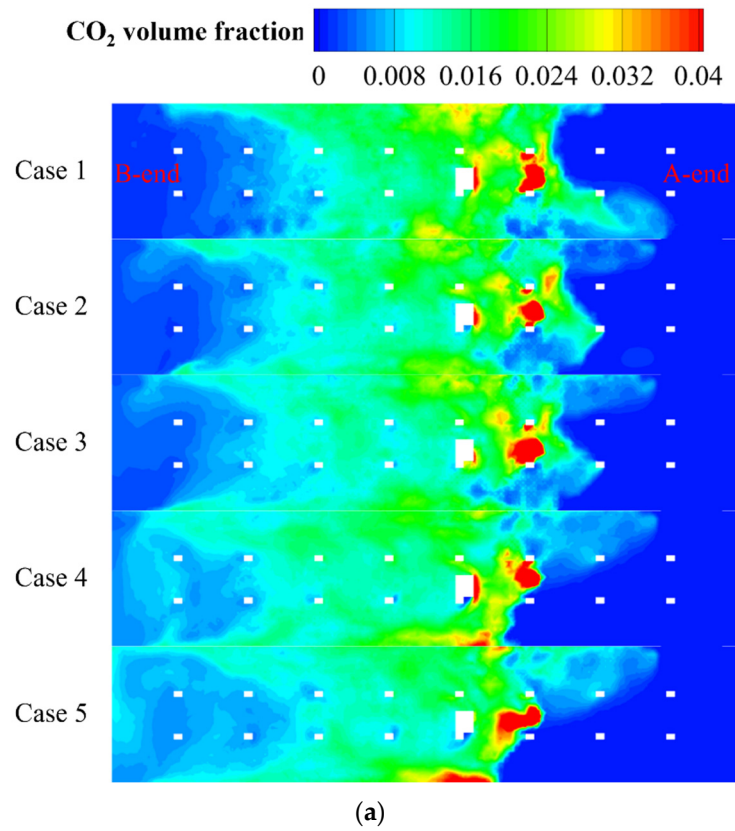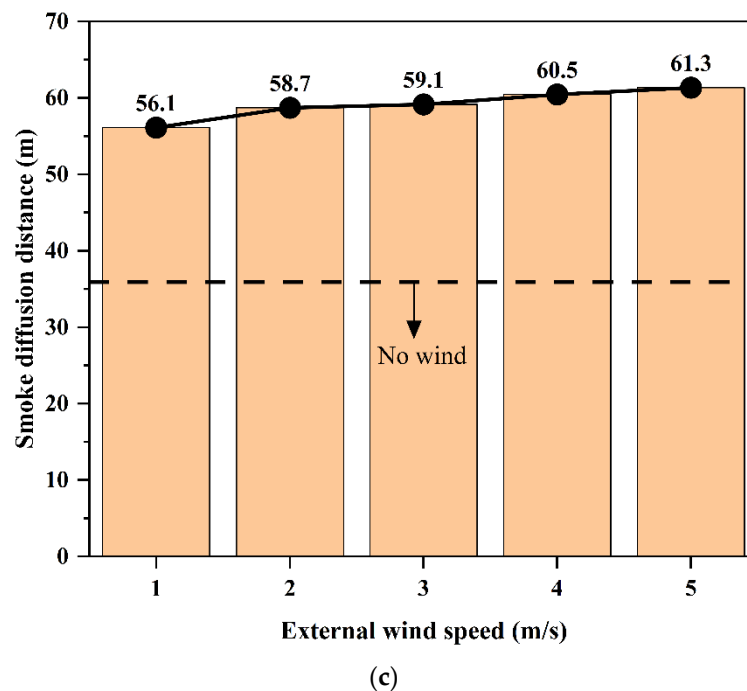
(**a**)

(**b**)

Figure 9. *Cont.*

(c)

Figure 9. Smoke concentration distribution characteristics in the station hall under different speeds of SSE wind. (**a**) Distribution contours, (**b**) longitudinal distribution, (**c**) diffusion distance.

3.2.2. N Wind

When the external wind direction was N, all entrances and exits were on the leeward side. Figure 10 displays the characteristics of the smoke concentration distribution over time in the station hall under Case 7. Figure 10a illustrates how the smoke gradually diffused symmetrically to both sides. Figure 10b demonstrates that when smoke first emerged at monitoring points C_{A10} and C_{B10} at about the same time, it did so at monitoring points C_{A20} and C_{B20} just 22 s later. According to the findings, smoke was largely dispersed towards the fire source center and spread constantly to both ends due to the combined effects of external wind and the TSE system.

As all three entrances were all on the leeward side, the impact of the external wind on the station hall was not immediately apparent. The station hall exhibited a state of negative pressure due to the suction of the TSE system, as seen in Figure 10c. Outdoor air entered the station hall through the three leeward entrances as a result of the difference in pressure between the inside and outside, and the corresponding wind speeds were 0.2 m/s, 0.19 m/s, and 0.29 m/s. Because the smoke grew over time and steadily got worse in the station hall, the TSE system was unable to quickly discharge it.

Figure 11 displays the influence of the N wind speed change from 1 to 5 m/s. The smoke diffused symmetrically to both sides, with the fire source as the center, as shown in Figure 11a. According to Figure 11b, the location of the CO_2 concentration center and the smoke concentration at A-end and B-end were similar to those in Case 0, indicating that the N wind direction had little impact on the spread of smoke. As seen in Figure 11c, the greatest smoke diffusion distance was 38.3 m, which represented an increase of just 4.76% over Case 0. Therefore, neither the direction nor the speed of the N wind had a major impact on the capability of the TSE system to control smoke.
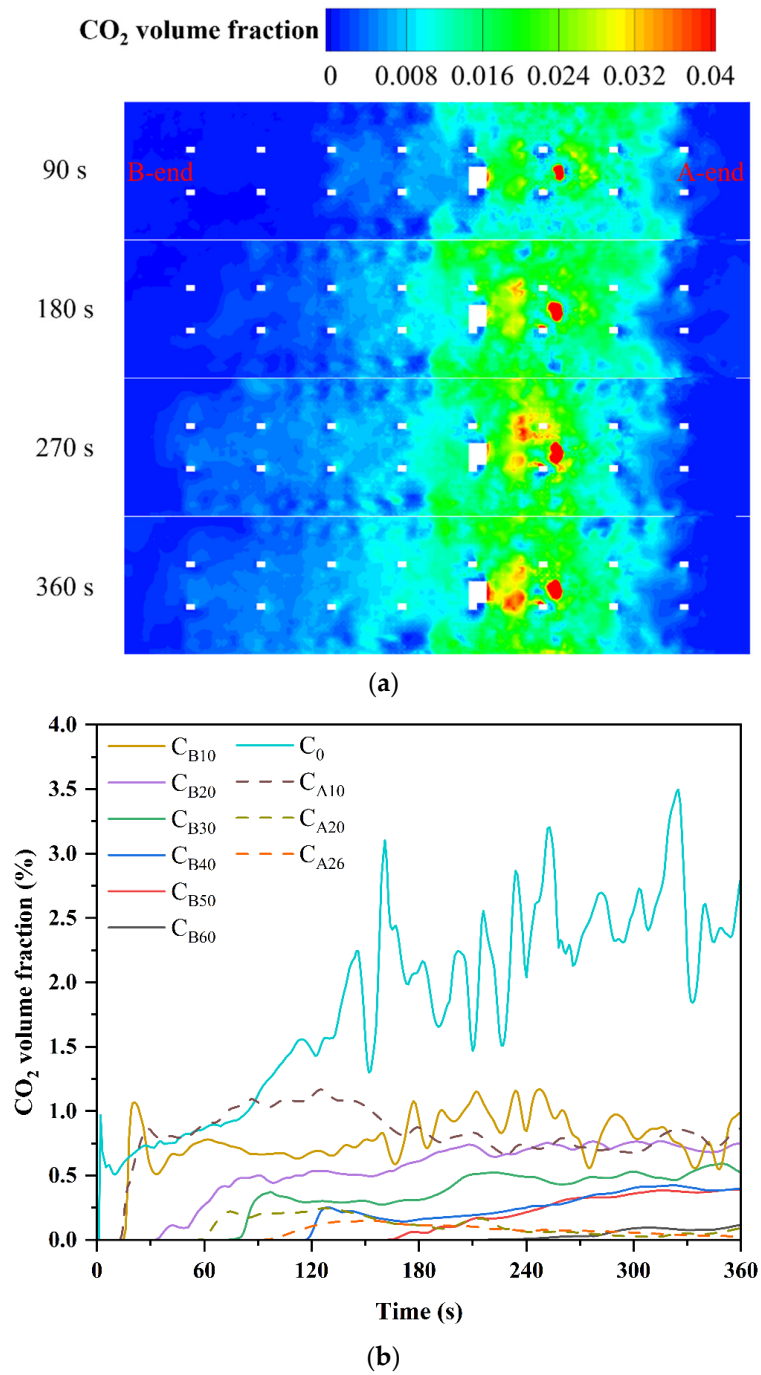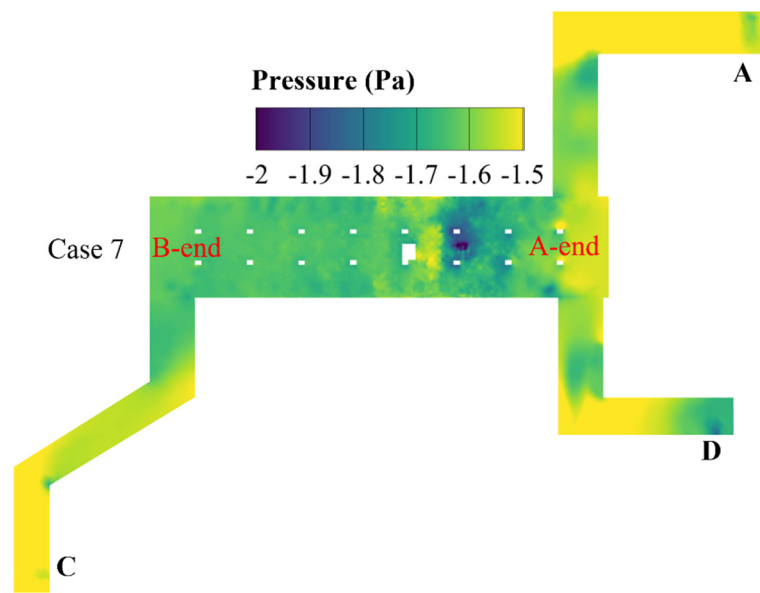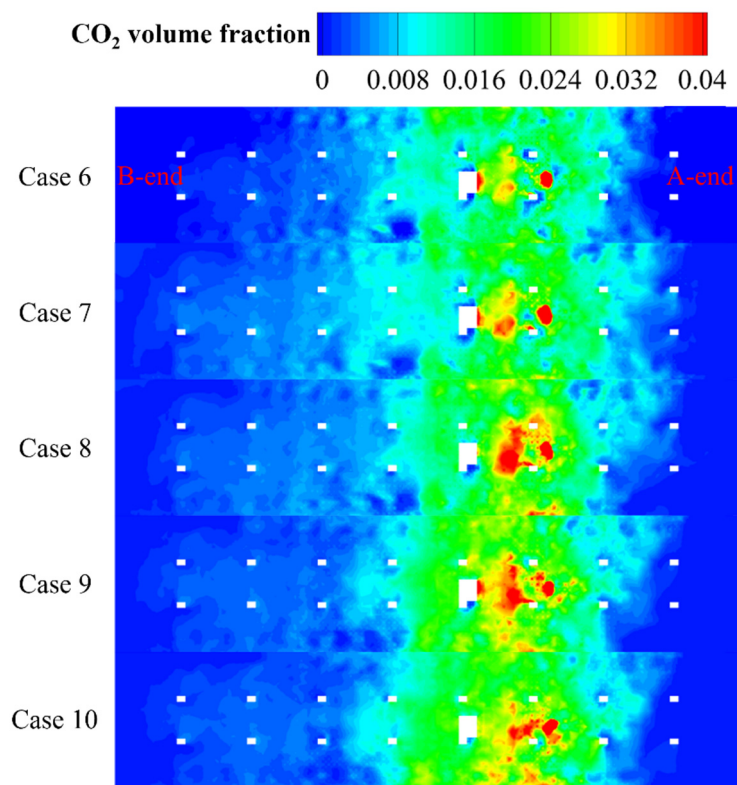
(**a**)

(**b**)

Figure 10. *Cont.*

(**c**)
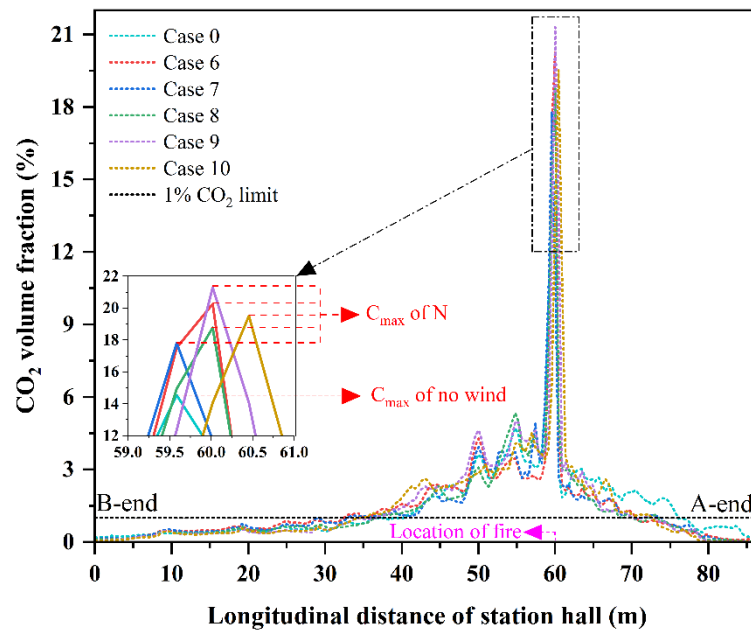
Figure 10. Smoke concentration distribution characteristics with time and pressure distribution contours in the station hall under Case 7. (**a**) Distribution contours, (**b**) variation at the monitoring points, (**c**) pressure distribution contour at 360 s.
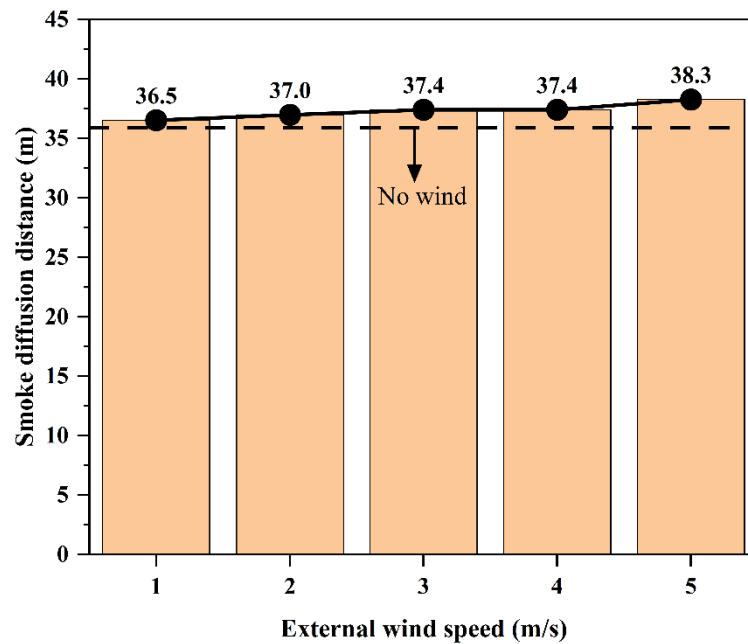

(**a**)

Figure 11. *Cont.*

(b)

(c)

Figure 11. Smoke concentration distribution characteristics in the station hall under different speeds of N wind. (**a**) Distribution contours, (**b**) longitudinal distribution, (**c**) diffusion distance.

3.2.3. SW Wind

When the external wind direction was SW, the entrances and exits of A and C were on the windward side, while the entrance and exit of D were on the leeward side. Figure 12 displays the characteristics of smoke concentration distribution over time under the Case 12 condition. As shown in Figure 12a, the smoke gradually spreads to both sides. Figure 12b demonstrates that the smoke spread to monitoring points C_{A10} (8 s), C_{A20} (28 s), and C_{A26} (44 s) sooner than it did to C_{B10} (22 s), C_{B20} (60 s), and C_{B30} (96 s), indicating that the smoke tended to diffuse toward the A-end under the influence of SW wind.

According to Figure 12c, the N wind caused a positive pressure at the entrances and exits A and C. Under the suction of the TSE system, the wind speed of the entrances and exits A and C was 0.25 m/s and 0.39 m/s, respectively. The entrance and exit D on the leeward side showed a negative pressure, with a pressure value lower than that in the station hall, and the corresponding wind speed was −0.1 m/s. The external wind caused the pressure gradient of the station hall to drop from passageways A and C to passageway D, which also contributed to the smoke's progressive spread to passageway D.

Figure 13 depicts the characteristics of the smoke concentration distribution in the station hall and passageway D under different SW wind speeds. Figure 13a illustrates how the smoke reached the A-end, as the windward side of the entrance and exit C caused the external wind to enter the station hall. As shown in Figure 13c, the smoke concentration near the fire source was the lowest in Case 0. The peak value of the smoke concentration grew gradually as the external wind speed increased, and it was closer to the A-end compared to elsewhere. This indicated that the N wind intensified smoke diffusion to the A-end. Figure 13d demonstrates that the greatest smoke diffusion distance was 37.0 m under the SW wind, which was similar to Case 0.
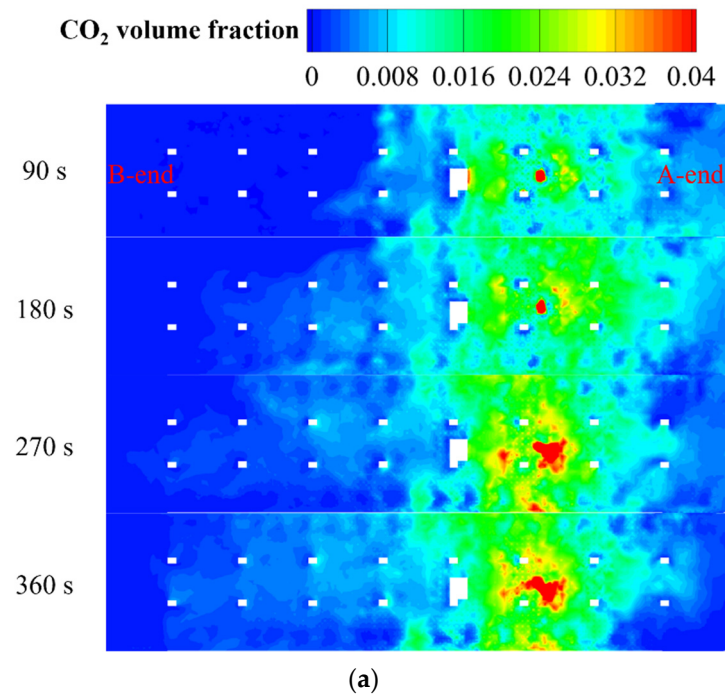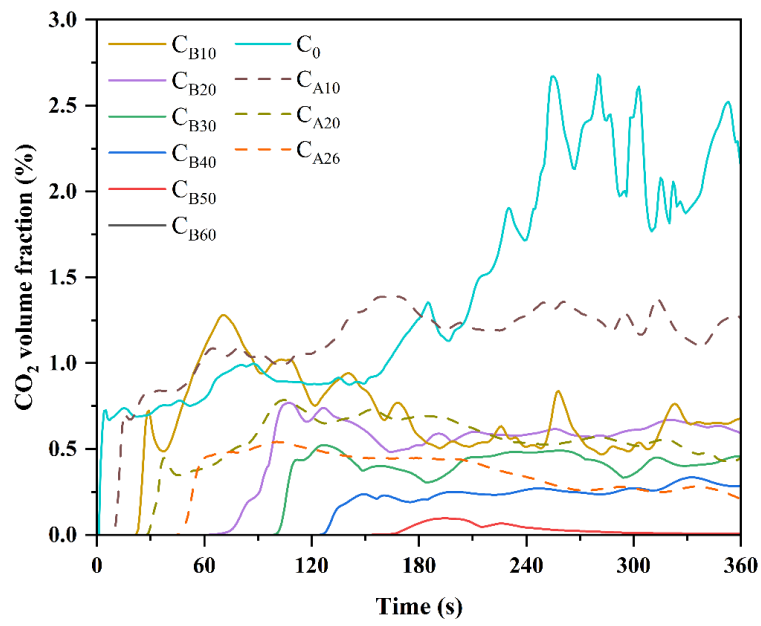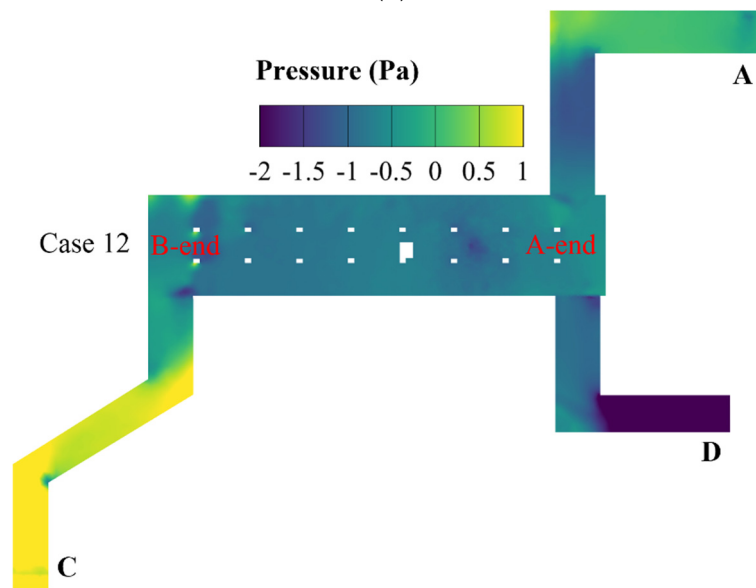

(**a**)

Figure 12. *Cont.*

(**b**)

(**c**)

Figure 12. Smoke concentration distribution characteristics with time and pressure distribution contours in station hall under Case 12. (**a**) Distribution contours, (**b**) variation at the monitoring points, (**c**) pressure distribution contour at 360 s.

(**a**)
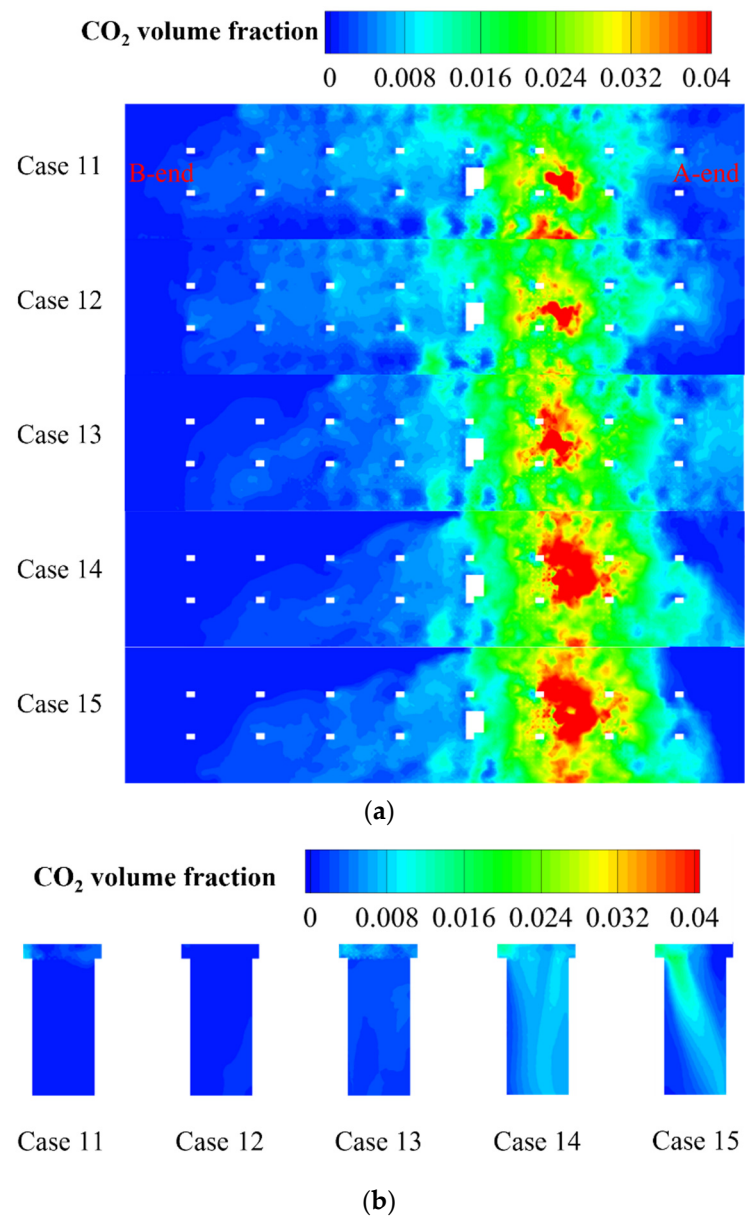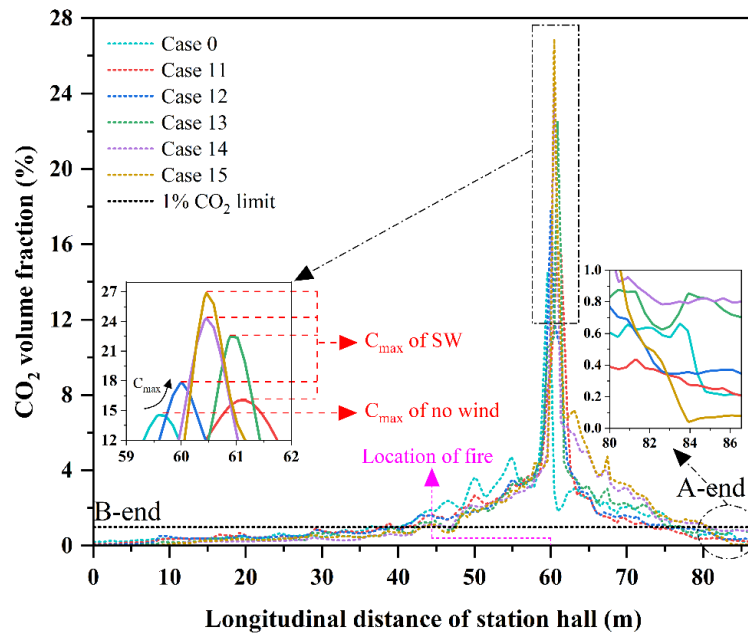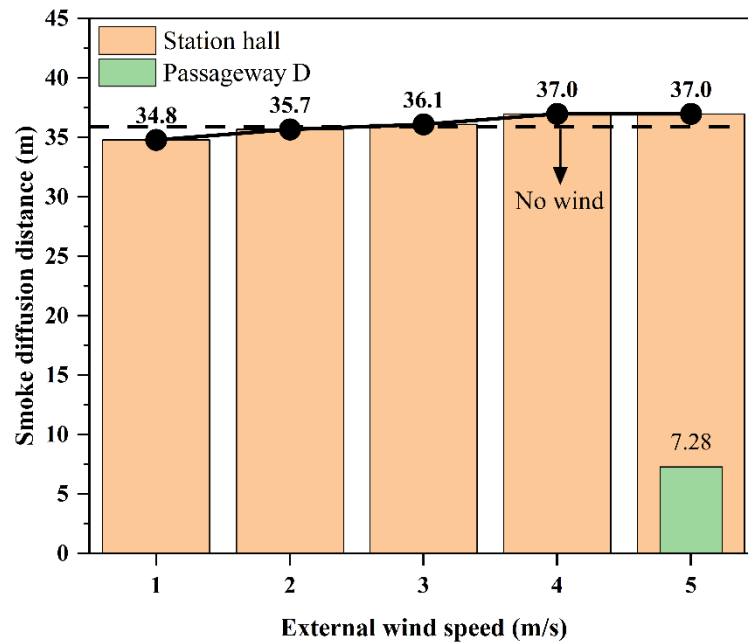

(**b**)

Figure 13. *Cont*.

(**c**)

(**d**)

Figure 13. Smoke concentration distribution characteristics in the station hall and passageway D under different speeds of SW wind. (**a**) Distribution contours of the station hall, (**b**) distribution contours of passageway D, (**c**) longitudinal distribution of the station hall, (**d**) diffusion distance of the station hall and passageway D.

When the wind speed was 5 m/s, the CO_2 concentration in passageway D exceeded 1%. As seen in Figure 13b, the opening of the TSE system direction was unable to completely prevent smoke from spreading to the passageways. Because of the influence of the draught between passageways A and D, the smoke at the A-end was carried to passageway D, which resulted in a drop in the CO_2 concentration at the A-end. From Figure 13d, it can be seen that the smoke diffusion distance of passageway D was 7.28 m at an external wind speed of 5 m/s.

3.3. Optimization of the Smoke Control System

The above study showed that the external wind had an impact on the characteristics of smoke concentration distribution under the TSE system. The smoke in the station hall diffused longitudinally to the B-end due to the SSE wind. The smoke spread to passageway D due to the SW wind's rapid speed, while the N wind had less of an impact. To solve the problem of the TSE system not being able to effectively control the smoke caused by the external wind, an OSC system with smoke barriers was proposed to implement the zoning control scheme in this study.

As shown in Figure 14, smoke barriers (0.5 m) were added to the passageways [24]. A central smoke barrier with a height of 1 m was installed on the middle ceiling of the station hall to divide the station hall into two smoke-control zones. To imitate the smoke control effect with the optimization measures, the least favorable conditions (Cases 5, 10, and 15) for each wind direction were selected as the control group. As shown in Table 6, the optimized working conditions were set as Cases 16, 17, and 18.
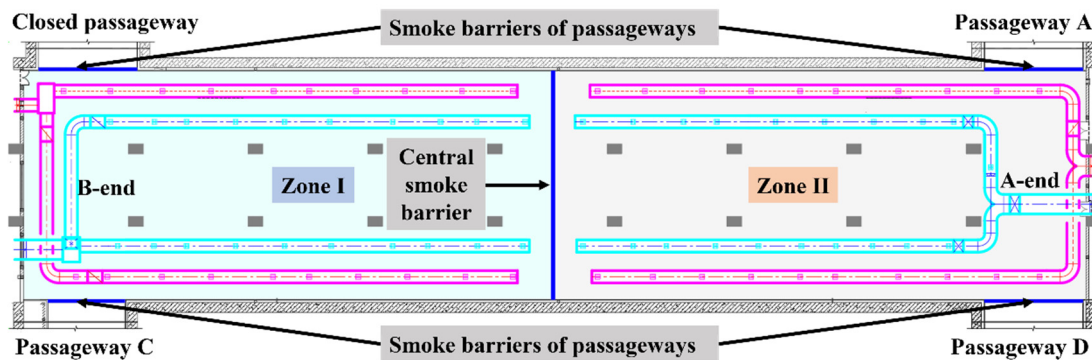

Figure 14. Schematic of the station hall with smoke barriers.

Table 6. Optimized simulation conditions.

Case	External Wind Direction	External Wind Speed (m/s)	Optimization Measure
16	SSE	5	Smoke barriers were installed in all
17	N	5	passageways and in the middle of the
18	SW	5	station hall

Figure 15 demonstrates how the three wind directions in Zone II effectively controlled the smoke. Figure 16 displays the characteristics of the CO_2 concentration distribution for the TSE and OSC systems under the three wind directions. Figure 16a illustrates how the smoke diffusion degree in Case 16 was significantly lower than that in Case 5. Compared to Case 10, the smoke diffusion degree in Case 16 decreased slightly, as shown in Figure 16b. This was mostly owing to the sudden change in smoke concentration caused by the intervention of the central smoke barrier, which effectively prevented smoke from spreading to Zone I. However, the peak value of the CO_2 concentration increased in the cases of the OSC system, owing to the accumulation of smoke above the fire source.
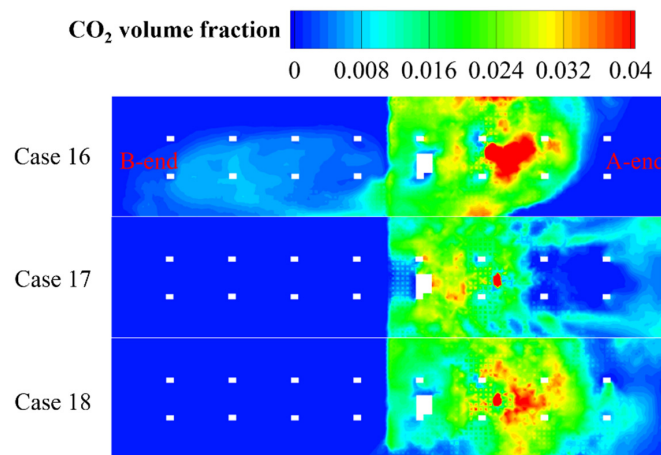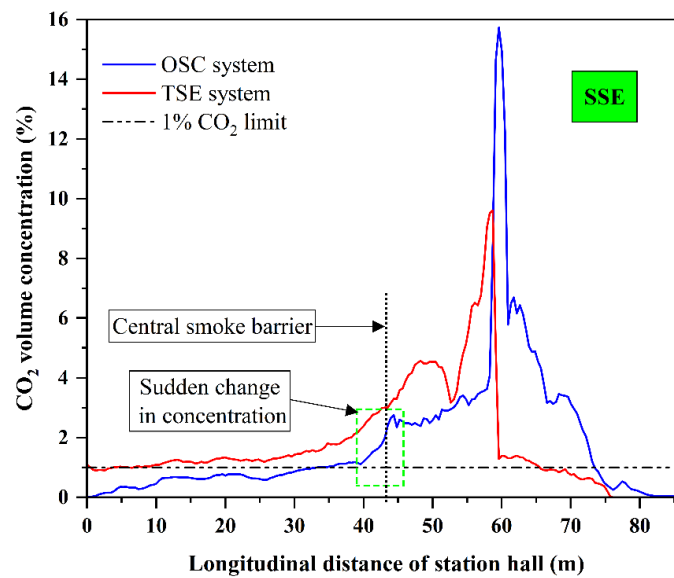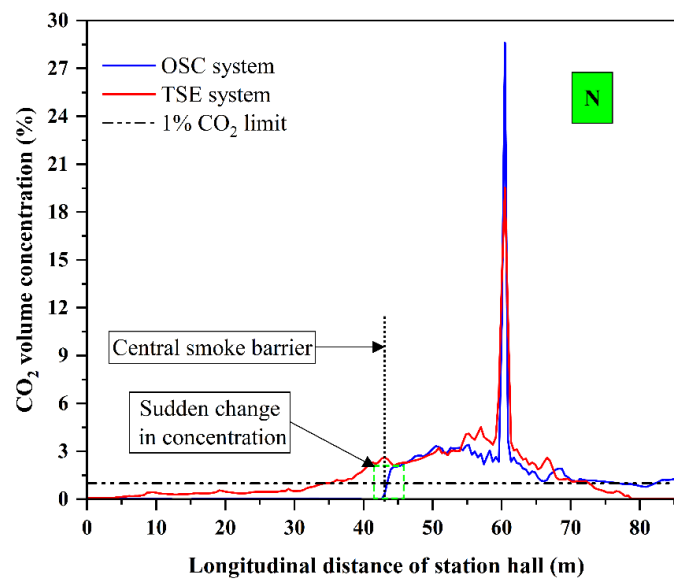
Figure 15. Smoke concentration distribution contours in the station hall under the OSC system.

(**a**)

(**b**)

Figure 16. *Cont.*
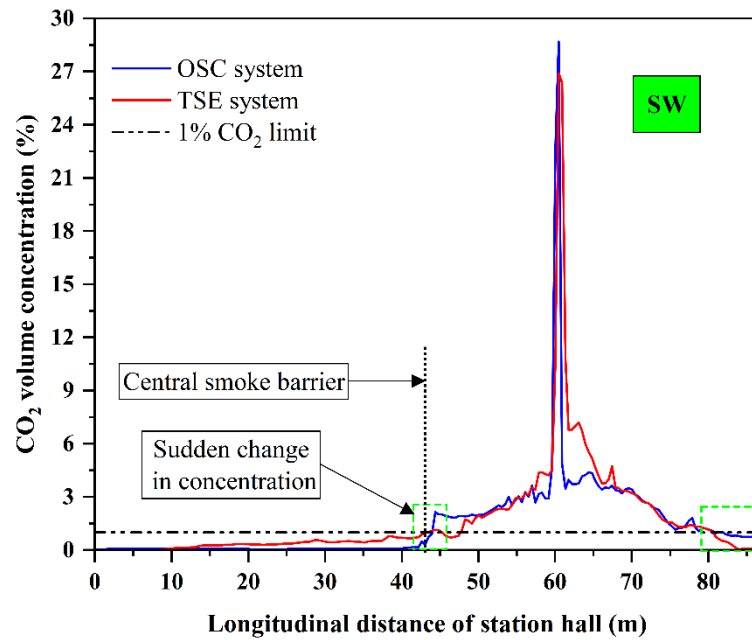
(c)
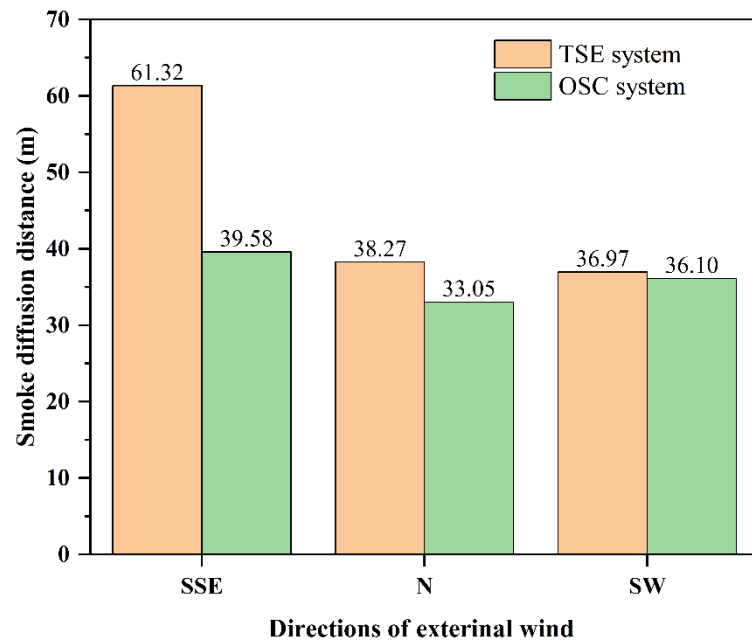
(d)

Figure 16. Comparison of smoke concentration distribution characteristics in the station hall under different wind directions between the TSE and OSC system. Longitudinal distribution under (**a**) SSE wind, (**b**) N wind, and (**c**) SW wind conditions, and (**d**) the diffusion distance.

According to the above research, preventing smoke from entering passageway D was the main purpose of the SW wind direction optimization. Figure 16c shows that the smoke diffusion distance of the station hall was not significantly shortened, and the CO_2 concentration at the A-end of the OSC system was greater than that of the TSE system. However, there was no smoke spread in any passageways during the entire evacuation period after the implementation of the TSE system. This was mainly due to the setting of smoke barriers at passageways, which directly obstructed the flow of smoke to passageway D. In Figure 16d, compared with the TSE system, the diffusion distances of the OSC system

were decreased by 21.74 m, 5.22 m, and 0.87 m, which correspond to differences of 35.45%, 13.64%, and 2.35%, respectively.

Adding smoke barriers to further divide the smoke control zones could effectively cope with the adverse impact of external wind on the TSE system in the station hall. The results showed that the smoke barrier in the passageways could prevent smoke from spreading to the passageways and outside air from flowing into the station hall, which lessened the impact of external wind on the smoke extraction in the station hall. The central smoke barriers had a specific impact on longitudinal diffusion, which effectively prevented the spread of smoke to the non-fire region and made it possible to evacuate safely.

4. Conclusions

In this study, a three-dimensional model of a station hall with an outside computational domain was established by considering an actual subway station as an example, and the accuracy of the numerical model was verified through field hot smoke testing. CFD was used to simulate the influence of the TSE system and smoke flow characteristics on the fire in the station hall under different external wind directions and speeds in Tianjin. In addition, the OSC system with smoke barriers was proposed, and the smoke exhaust efficiency of the OSC system was analyzed. The key findings are summarized as follows.

1. When all entrances and exits were on the windward side, the longitudinal diffusion problem of the station hall was severe, and smoke tended to spread to the side with fewer entrances and exits. With an increase in external wind speed, the longitudinal diffusion distance of the station hall increased, reaching a maximum diffusion distance of 61.32 m at 5 m/s, which was 67.9% greater than that under no wind.
2. When all entrances and exits were on the leeward side, the overall diffusion of smoke in the station hall was similar to that with no wind. The smoke in the station hall spread symmetrically with the fire source at the center and was not affected by the variation in the external wind speed. The longest smoke diffusion distance in the station hall at 5 m/s external wind speed was 38.27 m, which was only 4.76% longer than it was under no wind.
3. When two entrances and exits were on the windward side and the other on the leeward side, the smoke tended to spread to the entrances and exits located on the leeward side. As the external wind speed increased, the smoke diffusion distance in the station hall also increased. The longitudinal diffusion distance of the station hall at 5 m/s external wind speed was 36.97 m, which was similar to that with no wind; the smoke entered the passageway on the leeward side, and the longest diffusion distance was 7.28 m.
4. The OSC system can effectively shorten the longitudinal diffusion of smoke in the station hall and prevent smoke from spreading to passageways. Compared with the TSE system, the diffusion distances of the station hall were shortened by 35.45%, 13.64%, and 2.35%, respectively, and smoke diffusion did not occur in all passageways.

Author Contributions: Conceptualization, J.L., X.F., T.Y. and B.W.; methodology, J.L. and X.F.; software, J.L. and X.F.; validation, B.W.; formal analysis, J.L. and X.F.; investigation, T.Y. and E.X.; resources, B.W.; data curation, B.W.; writing—original draft preparation, J.L. and X.F.; writing—review and editing, T.Y. and Z.W.; visualization, J.L.; supervision, T.Y.; project administration, T.Y.; funding acquisition, T.Y. All authors have read and agreed to the published version of the manuscript.

Institutional Review Board Statement: Not applicable.

Informed Consent Statement: Not applicable.

Data Availability Statement: Not applicable.

Conflicts of Interest: The authors declare no conflict of interest.

Nomenclature

C_{An}	Concentration monitoring point, A represents the A-end of the fire source, and n represents the distance from the fire source
c_p	Isobaric specific heat capacity [J/(kg·K)]
C_s	Volume concentration of component s
D_s	Diffusion coefficient of component s (m²/s)
H	Net height of smoke extraction space (m)
H_s	The safe smoke height (m)
N	North
OSC	Optimized smoke control
P	Pressure (Pa)
S_s	Source term [kg/(m³·s)]
SSE	Southeast by south
S_T	Heat source [(kg·K)/(m³·s)]
S_u	Generalized source term (N/m³)
S_v	Generalized source term (N/m³)
S_w	Generalized source term (N/m³)
SW	Southwest
t	Time (s)
T	Temperature (K)
TSE	Traditional smoke extraction
u	Velocity vectors in the x-direction (m/s)
$\vec{v}$	Velocity vector (m/s)
v	Velocity vectors in the y-direction (m/s)
w	Velocity vectors in the z-direction (m/s)

Greek symbols

δ	Mean relative error (%)
λ	Thermal conductivity [W/(m·K)]
μ	Dynamic viscosity (N·s/m²)
ρ	Density (kg/m³)

Appendix A

The UDF file was expressed as follow:

```
#include "udf.h"
DEFINE_PROFILE(velo_profile,t,i)
{
real x[ND_ND];
face_t f;
begin_f_loop(f,t)
{
F_CENTROID(x,f,t);
F_PROFILE(f,t,i) = Vmax*pow((x [1]-11.4)/10,0.22);
}
end_f_loop(f,t)
}
```

References

1. Yin, H.; Yang, C.; Yi, L.; Yu, J.; Wu, Y.; Deng, Y.; Tang, Z. Ventilation and air conditioning system of deep-buried subway station in sub-tropical climates: Energy-saving strategies. *Appl. Therm. Eng.* **2020**, *178*, 115555.
2. Association CURT. Annual Statistics and Analysis Report on Urban Rail Traffic in 2021. Available online: https://www.camet.org.cn/tjxx/76472021 (accessed on 23 April 2022).
3. Stec, A.A.; Hull, T.R. *Fire Toxicity*; Woodhead Publishing Ltd.: Sawston, UK, 2010.
4. Li, S.C.; Huang, D.F.; Meng, N.; Chen, L.F.; Hu, L.H. Smoke spread velocity along a corridor induced by an adjacent compartment fire with outdoor wind. *Appl. Therm. Eng.* **2017**, *111*, 420–430.
5. Chen, J.; Zhong, M.; Cheng, H.; Long, Z.; Yang, Y. Model experimental study on fire in metro multi-line transfer station:(2) fire in cross-transfer station. *J. Saf. Sci. Technol.* **2020**, *16*, 5–11.

6.	Wu, J.; Wu, Z.; Cai, Z.; Liu, G.; Zhang, A. Study on propagation laws of smoke temperature in full-scale two-story island subway station hall. *J. Saf. Sci. Technol.* **2021**, *17*, 165–171.

7.	Zhao, D.; Jiang, J.; Zhou, R.; Tong, Y.; Wu, F.; Shi, L. Numerical study on the optimisation of smoke ventilation mode for interchange subway station fire. *Int. J. Vent.* **2016**, *15*, 79–93.

8.	Long, Z.; Liu, C.; Yang, Y.; Qiu, P.; Tian, X.; Zhong, M. Full-scale experimental study on fire-induced smoke movement and control in an underground double-island subway station. *Tunn. Undergr. Space Technol.* **2020**, *103*, 103508.

9.	Gao, R.; Li, A.; Hao, X.; Lei, W.; Zhao, Y.; Deng, B. Fire-induced smoke control via hybrid ventilation in a huge transit terminal subway station. *Energy Build.* **2012**, *45*, 280–289.

10.	Giachetti, B.; Couton, D.; Plourde, F. Smoke spreading analyses in a subway fire scale model. *Tunn. Undergr. Space Technol.* **2017**, *70*, 233–239.

11.	Giachetti, B.; Couton, D.; Plourde, F. Smoke spreading analysis from an experimental subway scale model. *Fire Saf. J.* **2016**, *86*, 75–82.

12.	Zhong, W.; Tu, R.; Yang, J.P.; Liang, T.S. A study of the fire smoke propagation in subway station under the effect of piston wind. *J. Civ. Eng. Manag.* **2015**, *21*, 514–523.

13.	Roh, J.S.; Ryou, H.S.; Park, W.H.; Jang, Y.J. CFD simulation and assessment of life safety in a subway train fire. *Tunn. Undergr. Space Technol.* **2009**, *24*, 447–453.

14.	Tsukahara, M.; Koshiba, Y.; Ohtani, H. Effectiveness of downward evacuation in a large-scale subway fire using Fire Dynamics Simulator. *Tunn. Undergr. Space Technol.* **2011**, *26*, 573–581.

15.	Park, W.H.; Kim, D.H.; Chang, H.-C. Numerical predictions of smoke movement in a subway station under ventilation. *Tunn. Undergr. Space Technol.* **2006**, *21*, 304.

16.	Zhong, M.; Liu, C.; Tian, X.; Xiao, Y.; Mei, Q.; Zhang, L. Full-scale experimental study on fire in one-platform-interchange elevated metro station-(2) station hall fire. *J. Saf. Sci. Technol.* **2018**, *14*, 5–12.

17.	Tian, X.; Zhong, M.; Chen, J.; Liu, C.; Qiu, P. Full-scale experimental study on cross transfer metro station: I. Station hall fire. *J. Saf. Sci. Technol.* **2019**, *15*, 11–18.

18.	Long, Z.; Liu, C.; Yang, Y.; Qiu, P.; Chen, J.; Zhong, M. Full-scale experimental study of a fire in an island subway station with a stepped hall. *J. Tsinghua Univ. Sci. Technol.* **2020**, *60*, 787–794.

19.	Zhang, X.; Ma, J.; Li, A.; Lv, W.; Zhang, W.; Li, D. Ventilation for subway stations with adjustable platform doors created by train-induced unsteady airflow. *Build. Environ.* **2019**, *152*, 87–104.

20.	Liu, S.M.; Pan, W.X.; Zhao, X.W.; Zhang, H.; Cheng, X.L.; Long, Z.W.; Chen, Q. Influence of surrounding buildings on wind flow around a building predicted by CFD simulations. *Build. Environ.* **2018**, *140*, 1–10.

21.	Henan Meteorological Bureau; Hubei Meteorological Bureau; Meteorological Observation Center of China Meteorological Administration; Heilongjiang Meteorological Bureau; Shandong Meteorological Bureau; Yunnan Meteorological Bureau; Hebei Meteorological Bureau; Shanxi Meteorological Bureau; Jilin Meteorological Bureau. *Specifications for Surface Meteorological Observation—Wind Direction and Wind Speed*; General Administration of Quality Supervision, Inspection and Quarantine of the People's Republic of China: Beijing, China, 2017; p. 16.

22.	Tominaga, Y.; Mochida, A.; Yoshie, R.; Kataoka, H.; Nozu, T.; Yoshikawa, M.; Shirasawa, T. AIJ guidelines for practical applications of CFD to pedestrian wind environment around buildings. *J. Wind Eng. Ind. Aerodyn.* **2008**, *96*, 1749–1761.

23.	Schmitt, F.G. About Boussinesq's turbulent viscosity hypothesis: Historical remarks and a direct evaluation of its validity. *C. R. Mec.* **2007**, *335*, 617–627.

24.	Fujun, W. *Computational Fluid Dynamics Analysis: PRINCIPLES and Applications of CFD Software*; Tsinghua University Press: Beijing, China, 2004.

25.	Yang, J.; Liu, M.; Zhang, H.; Zheng, W.; You, S.; Cui, T. Ventilation and energy performance study on platform screen doors with adjustable vents in a subway station. *Tunn. Undergr. Space Technol.* **2022**, *120*, 104291.

26.	Wang, Y.F.; Qin, T.; Sun, X.F.; Liu, S.; Jiang, J.C. Full-scale fire experiments and simulation of tunnel with vertical shafts. *Appl. Therm. Eng.* **2016**, *105*, 243–255.

27.	Liu, M.; Zhu, C.; Zhang, H.; Zheng, W.; You, S.; Campana, P.E.; Yan, J. The environment and energy consumption of a subway tunnel by the influence of piston wind. *Appl. Energy* **2019**, *246*, 11–23.

28.	Peng, Y.; Gao, Z.; Ding, W.; Zhang, J.; Li, X.; Xu, J.; Wei, Y. Application of computational fluid dynamics in subway environment without fire and smoke—Literature review. *Build. Environ.* **2021**, *206*, 108408.

29.	Xu, T.; Zhao, D.; Tao, H.; Lei, P. Extended CFD models for numerical simulation of tunnel fire under natural ventilation: Comparative analysis and experimental verification. *Case Stud. Therm. Eng.* **2022**, *31*, 101815.

30.	Zhang, L.M.; Wu, X.G.; Liu, M.J.; Liu, W.L.; Ashuri, B. Discovering worst fire scenarios in subway stations: A simulation approach. *Autom. Constr.* **2019**, *99*, 183–196.

31.	Shanghai Tunnel Engineering Rail Transit Design and Research Institute; Tianjin Fire Research Institute of Ministry of Public Security. *Standard for Fire Protection Design of Metro*; Ministry of Housing and Urban-Rural Development of the People's Republic of China: Beijing, China, 2018; p. 120.

32.	Hu, L.; Yang, P.; Lei, X.; Liu, Y. Numerical investigation on oscillations characteristics of self-excited thermoacoustic system forced by acoustic wave. *Appl. Energy* **2022**, *315*, 119028.

33. Beijing Urban Construction Design & Development Group Co. Limited. *Code for Design of Metro*; The State Standard of the People's Republic of China: Beijing, China, 2013; p. 643.

34. Meteorological Data Room of Meteorological Information Center of China; Meteorological Administration; Department of Architectural Technology and Science, Tsinghua University. *Special Meteorological Data Set for Building Thermal Environment Analysis in China*; China Architecture and Architecture Press: Beijing, China, 2005.

35. Yang, B.; Yang, C.; Ni, L.; Wang, Y.; Yao, Y. Field experiment on influence of cold protection technologies on thermal environment of subway station in severe cold region. *Build. Environ.* **2022**, *216*, 109055.

36. Zhang, X.; Hu, L.; Sun, X. Temperature profile of thermal flow underneath an inclined ceiling induced by a wall-attached fire. *Int. J. Therm. Sci.* **2019**, *141*, 133–140.

37. Chen, T.; Li, Y.; Xu, Z.; Kong, J.; Liang, Y.; Wang, B.; Fan, C. Study of the optimal pitch angle of jet fans in road tunnels based on turbulent jet theory and numerical simulation. *Build. Environ.* **2019**, *165*, 106390.

38. Sichuan Fire Research Institute of Men. *Technical Standard for Smoke Management Systems in Buildings*; Ministry of Housing and Urban-Rural Development of the People's Republic of China: Beijing, China, 2017; p. 137.

39. Zhong, M.H.; Zhang, X.K.; Liu, T.M.; Wei, X.; Fan, W.C. Safety evaluation of engineering and construction projects in China. *J. Loss Prev. Process Ind.* **2003**, *16*, 201–207.

40. Butcher, E.G.; Parnell, A.C. *Smoke Control in Fire Safety Design*; China Architecture and Architecture Press: Beijing, China, 1990.

41. Yingxin, Z.; Yinping, Z.; Xianting, L.; Youguo, Q.; Qingxuan, Z.; Borong, L. *Built Environment*; China Architecture & Building Press: Beijing, China, 2016.